



Published in final edited form as:

*J Refract Surg.* 2017 May 01; 33(5): 337–346. doi:10.3928/1081597X-20170126-02.

## Regeneration of defective epithelial basement membrane and restoration of corneal transparency

Gustavo K. Marino, MD<sup>1,2</sup>, Marcony R. Santhiago, MD, PhD<sup>2</sup>, Abirami Santhanam, PhD<sup>1</sup>, Andre A. M. Torricelli, MD, PhD<sup>2</sup>, and Steven E. Wilson, MD<sup>1</sup>

<sup>1</sup>Cole Eye Institute, Cleveland Clinic, Cleveland, Ohio

<sup>2</sup>University of Sao Paulo, Sao Paulo, Brazil

### Abstract

**PURPOSE**—To study regeneration of the normal ultrastructure of the epithelial basement membrane (EBM) in rabbit corneas that had -9D photorefractive keratectomy (PRK) and developed late haze (fibrosis) with restoration of transparency over one to four months after surgery and in corneas that had incisional wounds.

**METHODS**—Twenty-four rabbits had one of their eyes included into one of the two procedure groups (-9D PRK or nearly full-thickness incisional wounds), while the opposite eye serving as unwounded controls. All corneas were evaluated with slit lamp photos, transmission electron microscopy and immunohistochemistry for the myofibroblast marker alpha-smooth muscle actin and collagen type III.

**RESULTS**—In the ‘-9D PRK group’, corneas at one month after surgery had dense corneal haze and no evidence of regenerated EBM ultrastructure. By two months after surgery, however, small areas of stromal clearing began to appear within the confluent opacity (lacunae), and these corresponded to small islands of normally-regenerated EBM detected within larger area of the excimer laser-ablated zone with no evidence of normal EBM. By four months after surgery, the EBM was fully-regenerated and the corneal transparency was completely restored to the ablated zone. In the ‘Incisional wound group’, the two dense, linear corneal opacities were observed at one month after surgery and progressively faded by two and three months after surgery. The EBM ultrastructure was fully regenerated at the site of the incisions, including around epithelial plugs that extended into the stroma, by one month after surgery in all eyes.

**CONCLUSIONS**—In the rabbit model, spontaneous resolution of corneal fibrosis (haze) after high correction PRK is triggered by regeneration of EBM with normal ultrastructure in the excimer laser-ablated zone. Conversely, incisional wounds heal in rabbit corneas without the development of myofibroblasts because the EBM regenerates normally by one month after surgery.

---

Corresponding Author: Steven E. Wilson, MD, Cole Eye Institute, I-32, Cleveland Clinic, 9500 Euclid Ave, Cleveland, OH, United States, wilsons4@ccf.org.

**Proprietary interest statement:** None of the authors have any commercial or proprietary interest in this study.

## INTRODUCTION

In some situations, the wound healing response to corneal injury may lead to stromal fibrosis and a loss of corneal transparency (also referred to as haze) that compromises the normal function of the cornea to transmit and focus light. Myofibroblast generation and persistence have been identified as critical factors that lead to corneal stromal fibrosis.<sup>1-3</sup> These fibroblastic cells, naturally opaque due to their diminished crystallin protein production,<sup>1</sup> also produce disorganized extracellular matrix that disturbs the precise distribution and organization of the collagen fibers that are essential for corneal transparency.<sup>4</sup>

Defective epithelial basement membrane (EBM) regeneration has a critical role in modulating myofibroblast development and persistence.<sup>5, 6</sup> Restoration of the structural and functional integrity of the EBM after injury is the key determinant of whether a particular cornea maintains transparency or, alternatively, develops fibrosis after trauma, surgery, or infection. A normal EBM limits the passage of epithelium-derived growth factors such as transforming growth factor beta (TGF- $\beta$ ) and platelet-derived growth factor (PDGF) into the underlying stroma at sufficient levels to drive development of mature myofibroblasts from both keratocyte-derived and bone marrow-derived precursor cells and to inhibit myofibroblast apoptosis.<sup>7, 8</sup>

Prior studies applied transmission electron microscopy (TEM) to assess the ultrastructure of the EBM in rabbit corneas with and without corneal fibrosis in a photorefractive keratectomy (PRK) injury model.<sup>5</sup> The lack of normal EBM morphology (including the lamina lucida and lamina densa layers seen at the TEM level, for example at one month after high correction -9 diopters [D] PRK) in corneas with fibrosis (Fig. 1) contrasts with the regeneration of normal EBM with ultrastructure identical to that in unwounded control corneas at one month after lower correction, for example -4.5D PRK, in corneas that maintain transparency.<sup>5</sup> The purpose of the present study was to evaluate the correlation between late regeneration of the normal ultrastructure of the EBM and disappearance of myofibroblasts with restoration of transparency in corneas that developed fibrosis after PRK. EBM regeneration after nearly full-thickness incisional wounds was also analyzed in the rabbit model.

## MATERIALS AND METHODS

### Animals

Rabbits were selected for this study because of their well-characterized corneal wound healing response and the similarity of the PRK corneal fibrosis response in rabbits to that in human corneas.<sup>2,5,8</sup> Twenty-four 12- to 15-week-old female New Zealand white rabbits weighing 2.5 to 3.0 kg each had one of their eyes included in one of the two procedure groups (PRK or Incisional wounds), while the opposite eye was included as an unwounded control. All animals were treated in accordance with the tenets of the ARVO Statement for the Use of Animals in Ophthalmic and Vision Research. The Animal Control Committee at the Cleveland Clinic approved the animal study described in this work.

## Study groups and procedures

Rabbits were divided into two different groups: (1) -9D PRK or (2) Two linear, nearly full-thickness, non-perforating incisional wounds across the central cornea. The animals were sacrificed and had their corneas analyzed at different time points to characterize the corneal wound healing process using immunohistochemistry and transmission electron microscopy.

General anesthesia was obtained by intramuscular injection of ketamine hydrochloride (30 mg/kg) and xylazine hydrochloride (5 mg/kg). In addition, topical proparacaine hydrochloride 0.5% (Akorn Inc., Lake Forest, IL) was applied to both eyes at the time of the procedure.

The '-9D PRK group' underwent -9D PRK with 6 mm ablation zone using a VISX Star S4 IR excimer laser (Abbott Medical Optics, Irvine, CA). Briefly, a wire lid speculum was positioned in the eye and a 7mm diameter circle of central epithelium overlying the pupil was removed by scraping with a #64 Beaver blade (Beaver-Visitec International, Waltham, MA). A spherical excimer laser ablation was performed on the exposed stromal surface. One drop of ciprofloxacin hydrochloride 0.3% (Alcon) was instilled into the eye immediately after the procedure and continued twice a day until the epithelium was completely healed at four to five days after surgery. Three rabbits at each time point were euthanized at two weeks, and one, two, three, and four months after surgery.

Animals in the 'Incisional wound group' received two vertically-oriented linear nearly full-thickness (~350  $\mu$ m depth) incisional wounds across the central cornea with a 0.35mm depth guarded blade (Beaver-Visitec International, Waltham, MA). Ciprofloxacin hydrochloride 0.3% was instilled into the eye immediately after the procedure and continued twice a day until the epithelium was healed (three to four days). Three rabbits at each time point were euthanized after one, two, and three months after surgery.

Corticosteroids were not applied in any of the groups to avoid the potential confounding effects of these drugs on the corneal wound healing response.

## Tissue Fixation

Rabbits were euthanized with an intravenous injection of 100 mg/kg pentobarbital while the animals were under ketamine/xylazine general anesthesia. The corneoscleral rims of treated and unwounded eyes were removed without manipulation of the cornea using 0.12 mm forceps and sharp Westcott scissors (Fairfield, CT). The corneas were cut into two equal halves with a sharp single-edged razor and one half was immediately embedded in liquid optimal cutting temperature (OCT) compound (Sakura FineTek, Torrance, CA) within a 24 x 24 x 5 mm mold (Fisher Scientific, Pittsburgh, PA) and quickly frozen on a block of dry ice and stored at -80°C until sectioning was performed for immunohistological evaluation. The second corneal half was immediately stored in 2.5% glutaraldehyde and 4% paraformaldehyde with 0.2 M cacodylate buffer at 4°C.

For immunohistochemistry, central corneal sections (7  $\mu$ m thick) were cut within the excimer ablated or incisional zone with a cryostat (HM 505M; Micron GmbH, Walldorf, Germany) and placed on 25 x 75 x 1 mm microscope slides (Superfrost Plus; Fisher

Scientific, Pittsburgh, PA) and maintained at  $-80^{\circ}\text{C}$  until staining was performed. Sections within 0.5 mm of the razor bisection cut were not used in analyses to avoid the localized effects of this incision.

Sections were prepared for TEM by cutting 1 x 3 mm blocks of tissue perpendicular to the epithelial surface from both the excimer laser ablated zone, incisional zone or unwounded central corneas after the tissue had been fixed for 24 hours in TEM fixative. The excised blocks were replaced into the electron microscopy fixative and stored at  $4^{\circ}\text{C}$  until final sectioning.

### Immunohistochemistry

Immunohistochemistry was performed as previously described<sup>2</sup> to detect the alpha-smooth muscle actin ( $\alpha$ -SMA) marker for myofibroblasts or collagen type III (COL3)—a collagen type normally absent from normal corneas that is synthesized and deposited by activated cells in the new extracellular matrix formed during corneal wound healing.<sup>9</sup> Briefly, immunofluorescent staining for  $\alpha$ -SMA was performed using a mouse monoclonal anti-human  $\alpha$ -SMA clone 1A4 (Cat# M-0851, Dako, Carpinteria, CA). The slides were washed with PBS and incubated for 90 minutes at room temperature with anti- $\alpha$ -SMA antibody at 1:50 dilution in 1% BSA. Slides were then incubated at room temperature with secondary antibody, Alexa Fluor 568 goat anti-mouse IgG (Cat# A-11004, ThermoFisher Scientific, Rockford, IL) at a dilution of 1:100 in 1% BSA for 1 hour. COL3 was detected using a purified goat polyclonal antibody anti-human Collagen  $\alpha$ 1 Type III (sc-8781, Santa Cruz Biotechnology, Inc. Dallas, TX) that also recognized rabbit antigen. The antibody was used on the sections at 1:50 dilution in 5% donkey serum and incubated overnight at  $4^{\circ}\text{C}$ . Sections were washed with PBS and then incubated at room temperature for 60 minutes in donkey anti-goat IgG-FITC (sc-2024, Santa Cruz Biotechnology, Inc. Dallas, TX) secondary antibody at a dilution of 1:100 in 5% donkey serum.

Coverslips were mounted with Vectashield containing 4',6-diamidino-2-phenylindole (DAPI) (Vector Laboratories Inc., Burlingame, CA) to allow visualization of all nuclei in the tissue sections. Negative controls for COL3 were performed by the pre-absorption of the antibody with 10X concentration of the corresponding blocking peptide (sc-8781P, Santa Cruz Biotechnology, Inc. Dallas, TX), while negative controls for  $\alpha$ -SMA included non-specific antibody of the same isotype since no antigen was available for pre-absorption.<sup>3</sup>

The sections were analyzed and photographed with a Leica DM5000 microscope (Leica, Buffalo Grove, IL) equipped with Q-imaging Retiga 4000RV (Surrey, BC, Canada) camera and Image-Pro software (MediaCybernetics, Inc. Bethesda, MD).

### Transmission Electron Microscopy

TEM samples were prepared according to the protocol described by Fantes et al.<sup>10</sup> Briefly, specimens were placed in 2.5% glutaraldehyde and 4% paraformaldehyde with 0.2 M cacodylate buffer immediately after removal of the cornea and scleral rim, and then the specimens were immersed in the fixative for a minimum of 24 hours. Corneas then were rinsed with 0.2 M cacodylate buffer three times for 5 minutes each, post-fixed in 1% osmium tetroxide for 60 minutes at  $4^{\circ}\text{C}$ , and dehydrated in increasing concentrations of

ethanol from 30% to 95% for 5 minutes each at 4°C. Finally, dehydration was performed using three 10-minute rinses in 100% ethanol at room temperature and three 15-minute rinses with propylene oxide at room temperature. The excised blocks of central anterior cornea were then embedded in epoxy resin medium. One-micrometer-thick sections were stained with toluidine blue for orientation and light microscopy. Ultrathin 85 nm thick sections were cut with a diamond knife, stained with 5% uranyl acetate and lead citrate, and then observed using a Philips CM12 transmission electron microscope operated at 60 kV (FEI Company, Hillsboro, OR).

## RESULTS

### Slit-Lamp Evaluation

In the ‘-9D PRK group’, mild corneal haze was first observed at two weeks after surgery (Fig. 1B) and progressed to become dense haze at 1 month after surgery (Fig. 1C) in each cornea that was retained to one month or beyond. At two months after PRK, small areas of stromal clearing (*lacunae*) began to appear within the confluent corneal haze in the previously excimer laser-ablated zone (Fig. 2A). These *lacunae* progressively enlarged and coalesced over time to the point that the opacity was faint at three months after surgery (Fig. 2B). At four months, the corneal transparency of each -9D PRK cornea was fully restored (Fig. 2C).

In the ‘Incisional wound group’, all the corneas had two dense, linear corneal opacities at one month after surgery (Fig. 3A). These opacities progressively faded by two months and three months after surgery (Figs. 3B–C) but remained visible at the slit lamp.

### $\alpha$ -SMA+ Myofibroblasts

No  $\alpha$ -SMA+ myofibroblasts were observed in the control corneas with immunohistochemistry (Fig. 1D). In the ‘-9D PRK group’, only few  $\alpha$ -SMA+ myofibroblasts were observed in the subepithelial stroma of the ablated zone by two weeks after -9D PRK (Fig. 1E), whereas high densities of subepithelial  $\alpha$ -SMA+ myofibroblasts were observed at one month after surgery (Fig. 1F), which was the peak of myofibroblast anterior stromal density.<sup>2, 3</sup> The density of  $\alpha$ -SMA+ cells were decreased by two months after surgery (Fig. 2D). By three months after surgery, few, if any,  $\alpha$ -SMA+ myofibroblasts were noted in the subepithelial stroma of any section (minimum 30 stained per cornea) that was cut from the central cornea at this time point (Fig. 2E). No  $\alpha$ -SMA+ cells were observed in any -9D PRK corneal sections (minimum 30 per cornea) at 4 months after surgery (Fig. 2F).

Conversely, no  $\alpha$ -SMA+ myofibroblasts were observed in the stroma of any corneas in the ‘Incisional wound group’—either beneath the surface epithelium at the site of stromal penetration or along the epithelial plugs that extended into the stroma at time points from one to three months (Figs. 3D–F).

## Transmission Electron Microscopy

The corneal EBM in untreated control rabbit corneas had the normal ultrastructure found in rabbits and other species at magnifications over approximately 15,000X.<sup>11, 12</sup> The lamina lucida and lamina densa of the EBM appeared as continuous layers between basal epithelial cells and the anterior stroma—with a highly organized collagen fibrils and extracellular matrix in the anterior stroma (Fig. 1G).

All corneas analyzed at two weeks after -9D PRK had no evidence of regenerated lamina lucida or lamina densa within the ablated zone and visibly disordered extracellular matrix distributed in the anterior stroma (Fig. 1H). By 1 month after -9D PRK, there continued to be no evidence of regeneration of lamina lucida or lamina densa, and many cells appeared in the subepithelial stroma with the ultrastructural appearance of myofibroblast cells—large amounts of rough endoplasmic reticulum—and embedded in disorganized extracellular matrix (Fig. 1I). These cells were the  $\alpha$ -SMA+ cells noted in the anterior stroma in Fig. 1F. At two months after -9D PRK, there were fewer myofibroblasts noted in the subepithelial stroma and there were small islands of normal lamina lucida and lamina densa detected within larger areas with no evidence of regenerated EBM (Fig. 2G – transition of abnormal to normal EBM morphology). A continuous lamina densa and lamina lucida organization was noted throughout the excimer laser ablated zone at three months after -9D PRK in all corneas in this group (Fig. 2H). At four months after -9D PRK, fully-regenerated normal EBM with lamina lucida and lamina densa was noted in all corneas in this group and extracellular matrix in the anterior stroma was more organized without cells with characteristic myofibroblast morphology (Fig. 2I).

In the ‘Incisional wound group’, lamina lucida and lamina densa were fully regenerated beneath the epithelium at the incision and around epithelial plugs that extended into the stroma at all time points investigated—one month, two months, and three months. No  $\alpha$ -SMA+ cells were noted anywhere in the stroma at any time point in the incision group (Figs. 3D–F). The stromal extracellular matrix beneath and adjacent to these incisions was indistinguishable from that noted in unwounded control corneas (Figs. 3G–I), but there was hypercellularity of the stroma at the site of the incisions even at 3 months after surgery (Fig. 3D).

## Collagen type III

Immunofluorescent immunohistochemistry showed no COL3 staining in the control unwounded corneas (Fig. 1J). In the ‘-9D PRK group’, COL3 was detected in the subepithelial stroma of the ablated zone at two weeks after surgery (Fig. 1K). COL3 protein deposition in the subepithelial stroma areas increased from two weeks to 1 month (Fig. 1L) and from one to two months (Fig. 2J) after surgery, and then was stable at the three- and four-month time points (Figs. 2K and 2L) after surgery in all three corneas at these time points.

In the ‘Incisional wound group’, COL3 was present in the subepithelial stroma beneath the incisions at one month after surgery (Fig. 3J) and extended lateral to incisions for 50 to 100 microns in some corneas (not shown). Thus, the cornea between the parallel incisions

remained clear and had no COL3 deposition beneath the epithelium (not shown). COL3 deposition surrounded epithelial plugs extending into the stroma at two-months (Fig. 3K) and three-months (Fig. 3L) in all three corneas analyzed at each time point.

## DISCUSSION

Ultrastructural studies have demonstrated conclusively that defective regeneration of the EBM, including lamina lucida and lamina densa, is associated with the development of stromal fibrosis (haze) following injury or surgery.<sup>5, 6, 8</sup> The present study confirms this observation and demonstrates that the process of spontaneous resolution of fibrosis after an injury such as high correction -9D PRK correlates with eventual regeneration of the EBM. In the rabbit model, clear areas called *lacunae* that appear in the confluent fibrosis of the ablated stroma are areas where the normal EBM structure has been regenerated and underlying myofibroblasts have undergone apoptosis beginning at approximately two months after PRK surgery. These *lacunae*, and the normal regenerated EBM associated with them, expand and coalesce until the stromal fibrosis of the ablated zone disappears completely by four months after surgery. Similar development and spontaneous resolution of haze can be noted in human corneas after PRK, but the time course of the cycle is more prolonged. Peak late haze (fibrosis) in human corneas occurs at three to four months after surgery and complete resolution, if it occurs, typically is noted at one to two years after surgery.<sup>3</sup>

Myofibroblast development and persistence in the anterior stroma that is associated with stromal fibrosis is regulated by the balance of antagonistic growth factors that drive the generation and persistence (TGF- $\beta$  and PDGF) versus apoptosis (autocrine interleukin [IL]-1 of myofibroblasts or paracrine IL-1 from adjacent cells).<sup>13</sup> Thus, TGF- $\beta$  is a requisite driver of myofibroblast development and persistence, and blocks IL-1-stimulated myofibroblast apoptosis when it is present in the stroma at sufficiently high concentrations.<sup>4</sup> TGF- $\beta$  is constitutively (continuously) produced by the epithelium and its expression is upregulated after injury but it cannot penetrate into the stroma at sufficient levels to drive myofibroblast development from keratocyte-derived and bone marrow-derived precursor cells when structurally and functionally normal EBM is present.<sup>6, 7</sup> Once the epithelium and EBM are damaged or disrupted by infection, injury or surgery, however, epithelial TGF- $\beta$  is upregulated<sup>13</sup> and penetrates from the epithelium into the anterior stroma and initiates the development of myofibroblasts from both keratocyte-derived and bone marrow-derived precursor cells.<sup>6, 7</sup>

Recent studies in our laboratory have demonstrated conclusively that several components that make up the lamina lucida and lamina densa of normal EBM, such as nidogens and perlecan, are produced by both epithelial cells and keratocytes in both humans<sup>14</sup> and rabbits<sup>15, 16</sup> and production of these components is upregulated in stromal cells after epithelial injury.<sup>14</sup> Our working hypothesis is several of these components *must* be provided by keratocytes after the nascent anterior laminin layer is laid down by the healed epithelium.<sup>16, 17</sup> Laminins are principally responsible for initial organizing of basement membrane regeneration since they are uniquely able to self-assemble into sheet-like structures on cell surfaces,<sup>17</sup> and then other EBM components are gradually incorporated into the nascent

EBM—likely through interactive contribution by keratocytes or fibroblasts of components such as nidogens and perlecan to the posterior layers of the nascent EBM. After severe corneal injuries, such as high correction -9D PRK or microbial keratitis, where large numbers of keratocytes are killed via apoptosis and necrosis by the injury,<sup>2</sup> insufficient keratocytes are available in the subepithelial stroma to provide these critical components to regenerate the normal EBM during the immediate post injury period. Thus, the EBM remains structurally and functionally defective and layers of myofibroblasts (Fig 1I)—driven by resultant ongoing penetration of high levels of TGF $\beta$ —develop<sup>18</sup> in the anterior stroma to produce fibrosis (haze) and block peripheral and posterior keratocytes from repopulating the subepithelial stroma where they would facilitate EBM regeneration.

In contrast, minor injuries to the cornea, such as epithelial abrasion, epithelial debridement or low epithelial-stromal injury (–4.5D PRK, for example), cause only ephemeral disruption of the EBM, and keratocytes quickly repopulate the subepithelial stroma, EBM is fully-regenerated, and the vital penetration of epithelium-derived TGF- $\beta$  into the stroma is interrupted. Consequently, myofibroblast precursors that began development in the anterior stroma<sup>18</sup> undergo apoptosis before they can produce sufficient disordered extracellular matrix to disturb corneal transparency.

Once mature opaque<sup>1</sup> myofibroblasts become established in the subepithelial stroma, they secrete large amounts of abnormal extracellular matrix, including collagen type III (Figs. 1L, 2J, 2K and 2L) that is not normally present in the corneal stroma, and which alters the organization of the collagen lamellae to augment stromal opacity (Fig. 1C). Thus, a vicious cycle is established, with myofibroblasts being maintained by epithelium-derived TGF- $\beta$  in the absence of a normal functional EBM due to insufficient EBM component contributions from keratocytes that are blocked from moving into position where they could function to facilitate regeneration of the EBM. The TEM studies in the current study showed that, once established, the persistence of anterior stromal myofibroblasts is ended only when this pathophysiology is somehow interrupted by the full regeneration of structurally normal EBM. Thus, focal clear spots (termed *lacunae*, Figs. 2A and 2B) begin to appear within the confluent corneal haze at approximately two months after -9D PRK in the rabbit where normal EBM has been reassembled (Figs. 2G and 2H) and, thus, epithelium-derived TGF- $\beta$  levels declined to the point that underlying myofibroblasts underwent apoptosis.<sup>19</sup> These *lacunae*, initially localized and scattered, expand and coalesce over time until corneal transparency can be fully restored. The same process may occur in human corneas that develop late haze after PRK but the *lacunae* (Fig. 4) typically do not appear until one to two years after surgery.<sup>19</sup> This pattern of central spotty EBM repair and haze resolution, rather than centripetal EBM repair with haze clearing from the periphery of the excimer laser ablated stroma, is likely an important clue regarding the pathophysiology of the process. We hypothesize that this clearing is initiated by keratocytes that finally penetrate through the layers of subepithelial myofibroblasts, perhaps by localized induction of apoptosis of myofibroblasts via paracrine IL-1 release<sup>13</sup> to initiate repair of normal, fully-functional EBM in the spotty distribution revealed by the *lacunae*.

Importantly, cases of *breakthrough haze* (haze that develops despite administration of MMC after PRK) in humans typically have less tendency for spontaneous resolution<sup>3,4</sup> even three or



more years after surgery.<sup>3,19</sup> This is likely due to the decreased anterior keratocyte density or altered keratocyte function caused by the MMC treatment that compromises this keratocyte-driven restoration of transparency.<sup>4</sup>

In this rabbit model, COL3 remains in the anterior stroma (Figs. 2K and 2L) even once the EBM has been regenerated and the myofibroblasts have disappeared (Figs. 2H and 2I). It is possible the keratocytes that repopulated the stroma would have reabsorb this wound healing-associated collagen if sufficiently later time points had been studied.

The findings in this study for incisional nearly full-thickness wounds in rabbit confirm those of Jester and coworkers.<sup>20–22</sup> Thus, epithelial plugs extended into the stroma at the site of the incisional wounds, but no  $\alpha$ -SMA+ myofibroblast generation was noted from one to three months after the incisions (Figs. 3D, 3E, and 3F). Importantly, we noted regeneration of normal EBM beneath the epithelial plugs by one month after the incisions (Figs. 3G, 3H and 3K), and this is likely why myofibroblasts did not develop as they did after high-correction PRK, since the intact EBM would block TGF- $\beta$  penetration into the surrounding stroma at sufficient levels to drive myofibroblast development from precursor cells. Increased stromal cellularity, however, was noted at the site of the incisions (Figs. 3D, 3E and 3F) and COL3 was deposited in the stroma beneath the epithelial plugs (Figs. 3J, 3K, and 3L). COL3 is scarce or absent from the normal adult corneal stroma, but it is one of the earliest wound healing collagens to be laid down after corneal incision.<sup>21</sup> Thus, the opacity associated with these incisions in rabbit cornea is likely due to corneal fibroblasts derived from keratocytes, which are opaque like myofibroblasts due to their down-regulation of crystallins,<sup>1</sup> and the extracellular matrix secreted by these wound healing-associated stromal cells, including COL3. This healing of incisions without myofibroblast generation in rabbits is different from what has been reported in other species, including cats, monkeys and humans, where myofibroblasts have a prominent role.<sup>23–25</sup>

In summary, the corneal healing response after PRK is similar in the rabbit to what is noted in human corneas except a far greater percentage of rabbit corneas having high-correction PRK develop myofibroblast-derived fibrosis and the time course for fibrosis development and resolution is relatively compressed in the rabbit relative to the human. Conversely, incisional wounds in rabbit corneas heal without myofibroblast-derived fibrosis, but rather they heal with opacity attributable to  $\alpha$ -SMA- corneal fibroblasts.

## Acknowledgments

Supported by EY010056 and EY015638 from the National Eye Institute and Research to Prevent Blindness, New York, NY. This work utilized the *FEI Tecnai G2 Spirit* transmission electron microscope that was purchased with funding from National Institutes of Health SIG Grant 1S10RR031536-01.

We would like to thank Luciana L. Dibbin, PhD, Shanmugapriya Thangavadiivel, PhD, and Carla S. Medeiros, MD for help with immunohistochemistry and Mei Yin for help with transmission electron microscopy.

## References

1. Jester JV, Moller-Pedersen T, Huang J, et al. The cellular basis of corneal transparency: evidence for 'corneal crystallins'. *J Cell Sci.* 1999; 112:613–622. [PubMed: 9973596]

2. Mohan RR, Hutcheon AE, Choi R, et al. Apoptosis, necrosis, proliferation, and myofibroblast generation in the stroma following LASIK and PRK. *Exp Eye Res.* 2003; 76:71–87. [PubMed: 12589777]
3. Wilson SE. Corneal myofibroblast biology and pathobiology: generation, persistence, and transparency. *Exp Eye Res.* 2012; 99:78–88. [PubMed: 22542905]
4. Marino GK, Santhiago MR, Torricelli AA, Santhanam A, Wilson SE. Corneal Molecular and Cellular Biology for the Refractive Surgeon: The Critical Role of the Epithelial Basement Membrane. *J Refract Surg.* 2016; 32:118–125. [PubMed: 26856429]
5. Torricelli AA, Singh V, Agrawal V, Santhiago MR, Wilson SE. Transmission electron microscopy analysis of epithelial basement membrane repair in rabbit corneas with haze. *Invest Ophthalmol Vis Sci.* 2013; 54:4026–4033. [PubMed: 23696606]
6. Torricelli AA, Singh V, Santhiago MR, Wilson SE. The corneal epithelial basement membrane: structure, function, and disease. *Invest Ophthalmol Vis Sci.* 2013; 54:6390–6400. [PubMed: 24078382]
7. Barbosa FL, Chaurasia SS, Cutler A, et al. Corneal myofibroblast generation from bone marrow-derived cells. *Exp Eye Res.* 2010; 91:92–96. [PubMed: 20417632]
8. Netto MV, Mohan RR, Sinha S, Sharma A, Dupps W, Wilson SE. Stromal haze, myofibroblasts, and surface irregularity after PRK. *Exp Eye Res.* 2006; 82:788–797. [PubMed: 16303127]
9. Ljubimov AV, Saghizadeh M. Progress in corneal wound healing. *Prog Retin Eye Res.* 2015; 49:17–45. [PubMed: 26197361]
10. Fantes FE, Hanna KD, Waring GO 3rd, Pouliquen Y, Thompson KP, Savoldelli M. Wound healing after excimer laser keratomileusis (photorefractive keratectomy) in monkeys. *Arch Ophthalmol.* 1990; 108:665–675. [PubMed: 2334323]
11. Fujikawa LS, Foster CS, Gipson IK, Colvin RB. Basement membrane components in healing rabbit corneal epithelial wounds: immunofluorescence and ultrastructural studies. *J Cell Biol.* 1984; 98:128–138. [PubMed: 6368566]
12. Sta Iglesia DD, Stepp MA. Disruption of the basement membrane after corneal debridement. *Invest Ophthalmol Vis Sci.* 2000; 41:1045–1053. [PubMed: 10752940]
13. Kaur H, Chaurasia SS, Agrawal V, Suto C, Wilson SE. Corneal myofibroblast viability: opposing effects of IL-1 and TGF beta1. *Exp Eye Res.* 2009; 89:152–158. [PubMed: 19285499]
14. Torricelli AA, Marino GK, Santhanam A, Wu J, Singh A, Wilson SE. Epithelial basement membrane proteins perlecan and nidogen-2 are up-regulated in stromal cells after epithelial injury in human corneas. *Exp Eye Res.* 2015; 134:33–38. [PubMed: 25797478]
15. Santhanam A, Torricelli AA, Wu J, Marino GK, Wilson SE. Differential expression of epithelial basement membrane components nidogens and perlecan in corneal stromal cells in vitro. *Mol Vis.* 2015; 21:1318–1327. [PubMed: 26788024]
16. Santhanam A, Marino GK, Torricelli AAM, Wilson SE. Epithelial basement membrane (EBM) regeneration and changes in EBM component mRNA expression in stromal cells after corneal injury. *Mol Vision.* in press.
17. McKee KK, Harrison D, Capizzi S, Yurchenco PD. Role of laminin terminal globular domains in basement membrane assembly. *J Biol Chem.* 2007; 282:21437–21447. [PubMed: 17517882]
18. Chaurasia SS, Kaur H, de Medeiros FW, Smith SD, Wilson SE. Dynamics of the expression of intermediate filaments vimentin and desmin during myofibroblast differentiation after corneal injury. *Exp Eye Res.* 2009; 89:133–139. [PubMed: 19285070]
19. Torricelli AA, Santhanam A, Wu J, Singh V, Wilson SE. The corneal fibrosis response to epithelial-stromal injury. *Exp Eye Res.* 2016; 142:110–118. [PubMed: 26675407]
20. Busin M, Yau CW, Yamaguchi T, McDonald MB, Kaufman HE. The effect of collagen cross-linkage inhibitors on rabbit corneas after radial keratotomy. *Invest Ophthalmol Vis Sci.* 1986; 27:1001–1005. [PubMed: 3710725]
21. Cintron C, Hong BS. Heterogeneity of collagens in rabbit cornea: type VI collagen. *Invest Ophthalmol Vis Sci.* 1988; 29:760–766. [PubMed: 3130320]
22. Jester JV, Petroll WM, Feng W, Essepian J, Cavanagh HD. Radial keratotomy. 1. The wound healing process and measurement of incisional gape in two animal models using in vivo confocal microscopy. *Invest Ophthalmol Vis Sci.* 1992; 33:3255–3270. [PubMed: 1428701]

23. Garana RM, Petroll WM, Chen WT, et al. Radial keratotomy. II. Role of the myofibroblast in corneal wound contraction. *Invest Ophthalmol Vis Sci.* 1992; 33:3271–3282. [PubMed: 1428702]
24. Jester JV, Steel D, Salz J, et al. Radial keratotomy in non-human primate eyes. *Am J Ophthalmol.* 1981; 92:153–171. [PubMed: 7270627]
25. Melles GR, Binder PS, Moore MN, Anderson JA. Epithelial-stromal interactions in human keratotomy wound healing. *Arch Ophthalmol.* 1995; 113:1124–1130. [PubMed: 7661745]

Author Manuscript

Author Manuscript

Author Manuscript

Author Manuscript

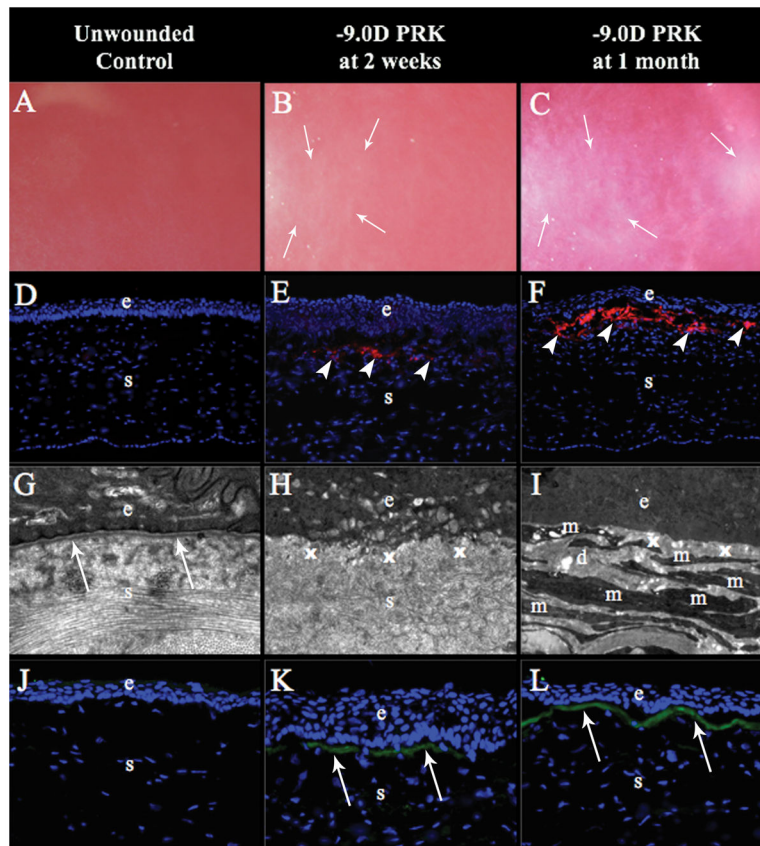


**Figure 1.**

Rabbit corneas that are unwounded, and at 2 weeks and 1 month after -9 diopters (D) photorefractive keratectomy (PRK). (A) Control corneas were clear without any haze (mag 25X). (B) Mild haze restricted to the area of excimer laser ablation was noted in all corneas at two weeks after the ablation (mag 25X). (C) Dense subepithelial haze was observed at one month after PRK (mag 25X). (D) Control corneas had no alpha-smooth muscle actin ( $\alpha$ -SMA)+ cells (mag 200X). (E) Corneas had a few  $\alpha$ -SMA+ cells (arrowheads) in the excimer laser ablated zone at two weeks after -9D PRK (mag 200X). (F)  $\alpha$ -SMA+ cells (arrowheads) were present at high density in the subepithelial excimer laser-ablated zone in all corneas after 1 month (mag 200X). (G) Transmission electron microscopy (TEM) of control corneas showed normal epithelial basement membrane (EBM) lamina densa (arrows) and lamina lucida, and normal organized extracellular matrix (mag 23,000X). (H) At two weeks after -9D PRK, there was no detectible lamina lucida and lamina densa where EBM is normally noted (x) within the excimer laser ablated zone and disorganized extracellular matrix was prominent in the subepithelial stroma (s) (mag 23,000X). (I) At one month after -9D PRK, no lamina lucida or lamina densa were detected within the excimer laser ablated zone where EBM would be detected (x) and there were layers of cells (m) with large amounts of rough endoplasmic reticulum that correspond to the  $\alpha$ -SMA+ cells (myofibroblasts) in Fig. 1F embedded in disorganized extracellular matrix (d) (mag 23,000X). (J) Control corneas had no detectible collagen type III (COL3) (mag 400X). (K) At two weeks after -9D PRK, corneas had COL3 (arrows) in the subepithelial stroma (mag 400X). (L) At one month after

-9D PRK, all corneas had greater COL3 (arrows) in the subepithelial stroma (mag 400X).  
Blue is DAPI staining of cell nuclei; (e) epithelium; (s) stroma.

Author Manuscript

Author Manuscript

Author Manuscript

Author Manuscript

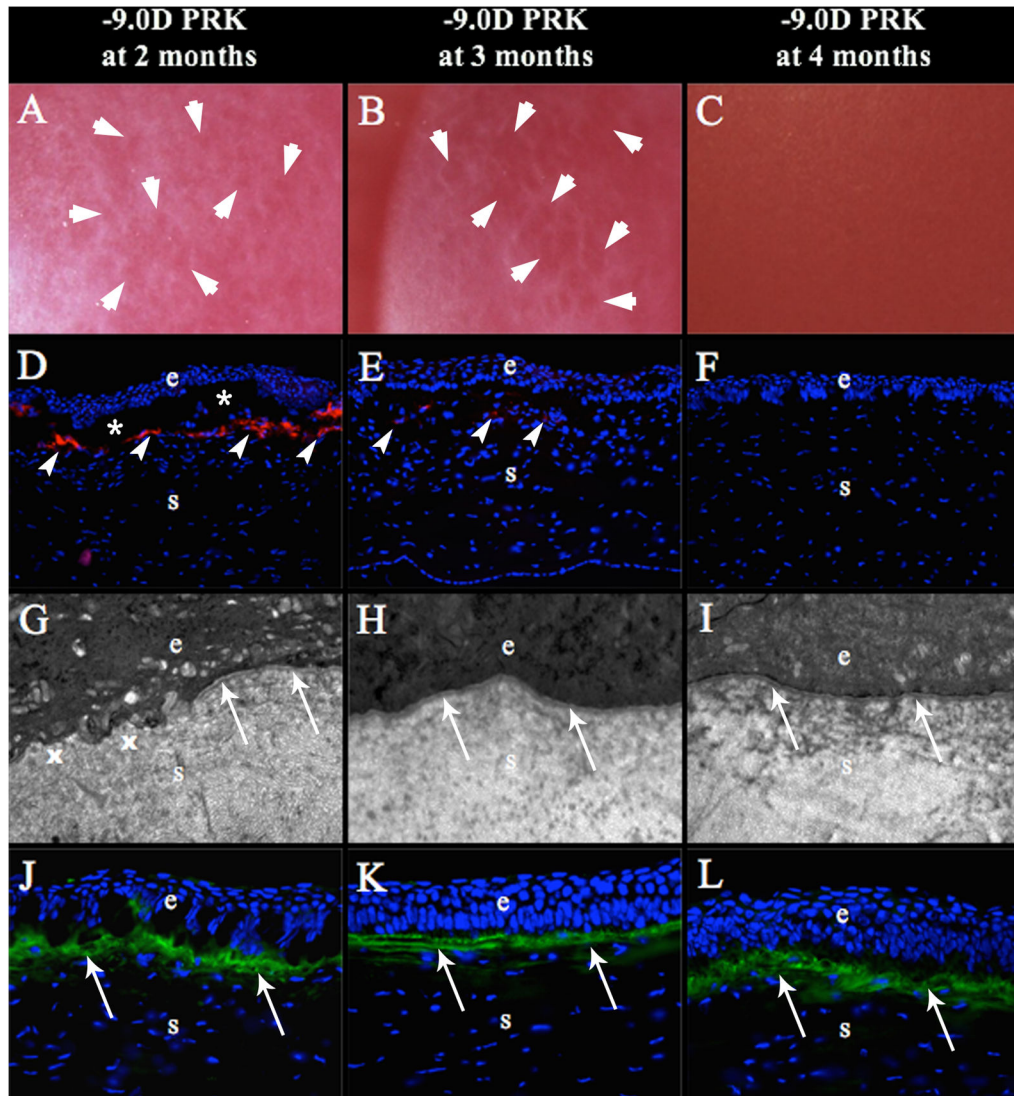


**Figure 2.**

Rabbit corneas at two months, three months and four months after -9 diopters (D) photorefractive keratectomy (PRK). (A) At two months after -9D PRK, all the corneas had developed some clear areas called “*lacunae*” (arrows) within the confluent corneal haze in the excimer laser ablated zone (mag 25X). (B) At three months after -9D PRK, *lacunae* (arrows) had enlarged and began to coalesce in all corneas (mag 25X). (C) At four months after -9D PRK, corneal transparency was fully restored in all corneas (mag 25X). (D) At two months after -9D PRK, large numbers of  $\alpha$ -SMA+ myofibroblasts (arrowheads) were present in the subepithelial stroma, although less than corneas at one month after PRK (mag 200X). (\*) represents artifactual detachment of the epithelium from stroma that occurred during sectioning. (E) At three months after -9D PRK, there were few remaining  $\alpha$ -SMA+ myofibroblast (arrowheads) in the subepithelial stroma within the excimer laser ablated zone (mag 200X). (F) At four months after -9D PRK, there were no remaining  $\alpha$ -SMA+ myofibroblasts in the subepithelial stroma (mag 200X). (G) At two months after -9D PRK, transmission electron microscopy (TEM) of the excimer laser ablated zone showed areas of

fully-regenerated EBM (arrows) with lamina lucida and lamina densa adjacent to areas without normal EBM (x) in all corneas at this time point (mag 23,000X). (H) At three months after -9D PRK, normal EBM (arrows) was regenerated in the excimer laser ablated zone in all corneas (mag 23,000X). (I) At four months after -9D PRK, normal EBM was regenerated in the excimer laser ablated zone in all corneas (mag 23,000X). (J) At 2 months after -9D PRK, large amounts of collagen type III (COL3, arrows) were detected in subepithelial stroma of the ablated zone of all corneas (mag 400X). The amount of COL3 in the subepithelial stroma appeared unchanged at three months (K) and four months (L) after -9D PRK (mag 400X). Blue is DAPI staining of cell nuclei; (e) epithelium; (s) stroma.

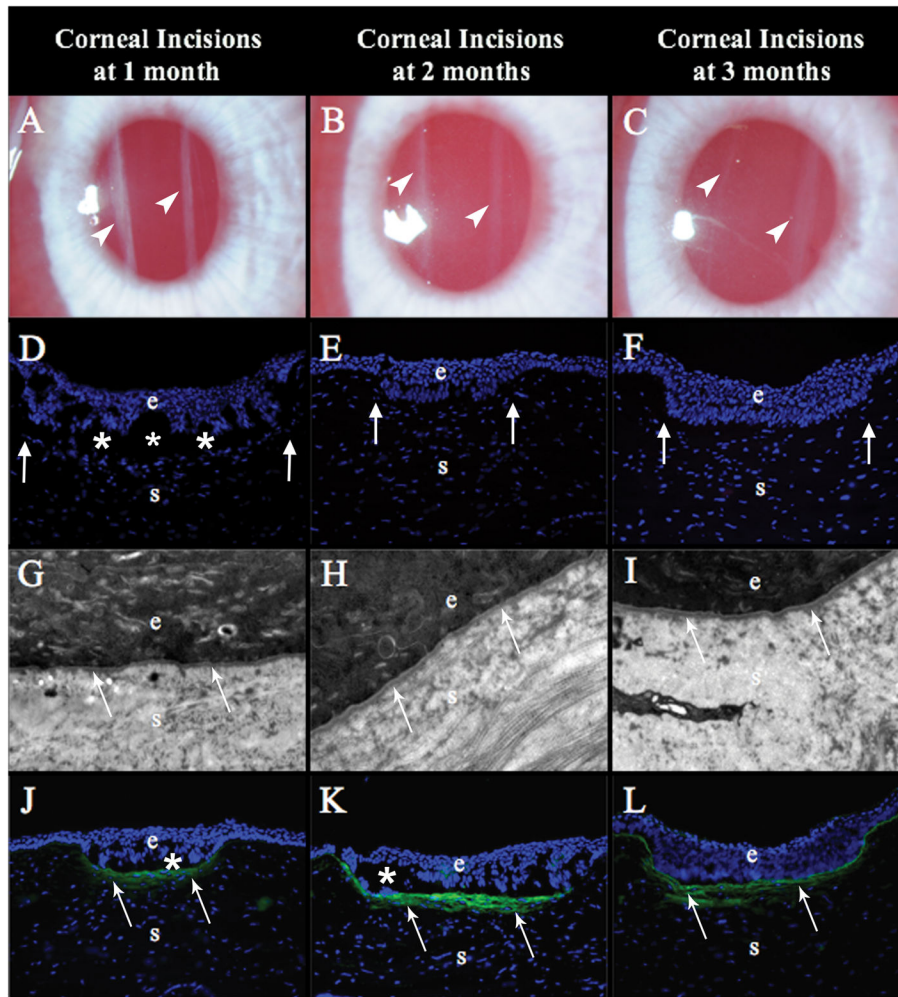


**Figure 3.** Rabbit corneas at one, two and three months after non-perforating linear incisions. (A) At one month after the surgery, the two incisions (arrowheads) were visible as dense linear opacities in all nine corneas that reached this time point (mag 25X). (B) At two months after surgery, the incisions (arrowheads) were less opaque in all six corneas that reached this time point (mag 25X). (C) At three months after surgery, the incisions (arrowheads) were faint compared to the two-month time point in all three corneas that reached this time point (mag 25X). (D), (E), and (F) At one, two or three months after surgery, respectively, there were no alpha-smooth muscle actin ( $\alpha$ -SMA)+ cells anywhere in the cornea, including around the epithelial plugs (arrows), in three corneas at each time point (mag 200X). (G), (H), and (I) At one, two and three months, respectively, after surgery the EBM (arrows), including lamina lucida and lamina densa, were fully regenerated and surrounded the epithelial plugs in all three corneas at each time point (mag 23,000X). (J) At 1 month after surgery, both incision in each of the three corneas studied had collagen type III (COL3, arrows) deposited in the subepithelial stroma beneath the epithelial plugs (mag 200X). At two months (K) and three months (L) after surgery, more COL3 deposition (arrows), compared to the one month time point, was noted in the subepithelial stroma surrounding the epithelial plugs in each of



the three corneas at each time points. Blue is DAPI staining of cell nuclei; (e) epithelium; (s) stroma; (\*) indicates artifact separation of the epithelium from the stroma that occurs during cutting of the section.

Author Manuscript

Author Manuscript

Author Manuscript

Author Manuscript

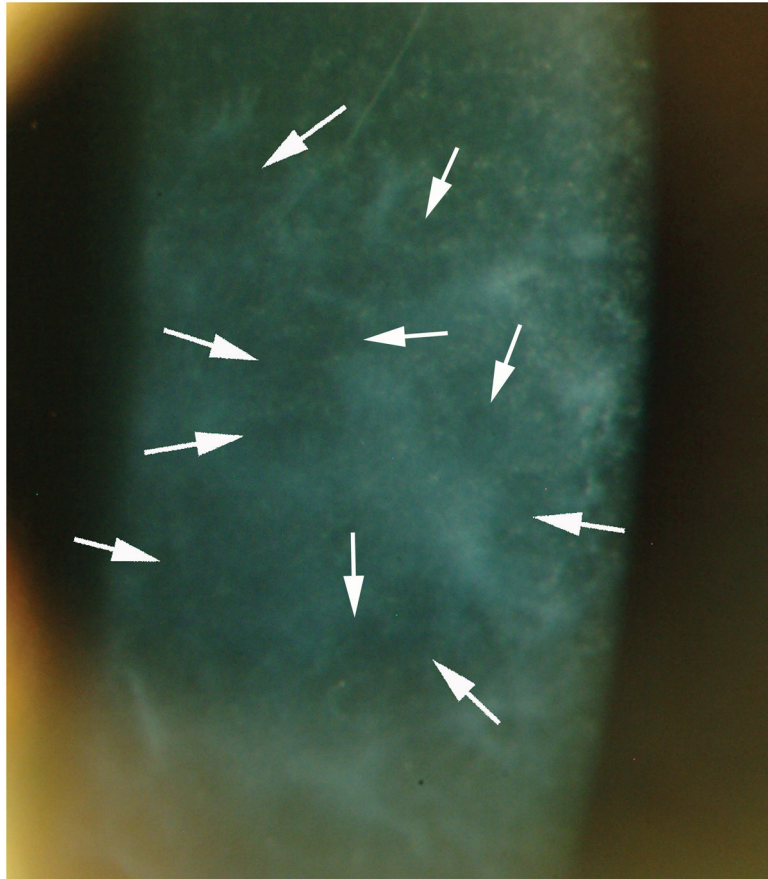


**Figure 4.** Human cornea with severe late haze at one and a half years after photorefractive keratectomy (PRK) for high myopia in which mitomycin C was not used after surgery. Arrows indicate clear “*lacunae*” appearing in the haze. These *lacunae* continued to enlarge and coalesce until the cornea was clear by three years after PRK (not shown). Mag 20X. (Reprinted in part by permission from Torricelli, Santhanam, Wu, Singh, and Wilson. *Exp Eye Res* 2016; 142:110–118).